



Optimized phospholipid-based nanoparticles for inner ear drug delivery and therapy



Keum-Jin Yang^{a,1}, Jihwan Son^{b,1}, So Young Jung^a, Gawon Yi^b, Jihye Yoo^b,
Dong-Kee Kim^{c,*}, Heebeom Koo^{b,d,**}

^a Clinical Research Institute, Daejeon St. Mary's Hospital, College of Medicine, The Catholic University of Korea, Daejeon, Republic of Korea

^b Department of Medical Lifescience, College of Medicine, The Catholic University of Korea, Seoul, Republic of Korea

^c Department of Otolaryngology, Daejeon St. Mary's Hospital, College of Medicine, The Catholic University of Korea, Daejeon, Republic of Korea

^d Catholic Photomedicine Research Institute, College of Medicine, The Catholic University of Korea, Seoul, Republic of Korea

ARTICLE INFO

Article history:

Received 16 January 2018

Received in revised form

26 March 2018

Accepted 14 April 2018

Available online 16 April 2018

Keywords:

Inner ear
Drug delivery
Nanoparticle
Hearing loss
Ototoxicity
Dexamethasone

ABSTRACT

To develop efficient carriers for inner ear drug delivery, we prepared four kinds of phospholipid-based nanoparticles: neutral, anionic, cationic, and cationic-PEG (polyethyleneglycol) particles. PEG was used to maintain long-term particle circulation in the perilymph, avoiding non-specific binding of particles to proteins. All four nanoparticles were about 200 nm in diameter, and their zeta potentials were -4.32 , -26.0 , $+25.8$, and -0.28 , respectively, for neutral, anionic, cationic, and cationic-PEG nanoparticles. To test particle efficacy *in vitro*, we used an artificial mucosa 100 μm in thickness to model the round window membrane (RWM) and HEI-OC1 cells, which were treated with particles containing Nile Red dye. Based on the levels of particle penetration and cellular uptake in this model system, we selected an optimal particle for further study. We also observed the movement of particles in *ex vivo* organotypic cultures of the organ of Corti. In mice, we analyzed the biodistribution of dexamethasone (Dex) in the inner ear after intratympanic injection of Dex-loaded nanoparticles. Then, we tested the therapeutic utility of the Dex-loaded nanoparticles in a mouse model of ototoxicity. In the auditory brainstem response (ABR) test, particle provided improved hearing loss recovery at all tested frequencies, more so than did the Dex sodium phosphate (Dex-SP) solution in current clinical use. Furthermore, quantitative PCR showed that nanoparticles reduced the levels of pro-inflammatory cytokines, exhibiting anti-inflammatory effects superior to those of Dex-SP. Thus, the surface properties of nanoparticles play pivotal roles in particle penetration and distribution after intratympanic injection. Our *in vitro* screening system using an artificial mucosa will also be valuable in the development of carriers for inner ear drug delivery.

© 2018 Elsevier Ltd. All rights reserved.

1. Introduction

Hearing loss is a common feature of many inner ear diseases and its prevalence is increasing. However, treatment of most inner ear

diseases remains intractable, partly because drugs do not readily reach the inner ear. When a drug is administered systemically, the biggest obstacle to inner ear absorption is the blood-labyrinth barrier (BLB) [1]. To overcome this problem, intratympanic drug injection has become part of the standard treatment for Meniere's disease and sudden deafness [2,3]. However, the concentrations of drugs in the inner ear remain low even after intratympanic drug injection. Several methods have been proposed to improve the efficacy of such injection, including nanoparticle-mediated delivery. In theory, nanoparticle-based drug delivery would enhance drug availability in the inner ear and release drugs in a sustained manner [4].

In recent years, rather than simply investigating the permeation of nanoparticles into the inner ear, a growing number of reports

* Corresponding author. Department of Otolaryngology-Head and Neck Surgery, Daejeon St. Mary's hospital, College of Medicine, The Catholic University of Korea, Daeheung-dong, Jung-gu, Daejeon, Republic of Korea.

** Corresponding author. Department of Medical Lifescience, College of Medicine, The Catholic University of Korea. 222 Banpo-daero, Seocho-gu, Seoul, 06591, Republic of Korea.

E-mail addresses: cider12@catholic.ac.kr (D.-K. Kim), hbkooc@catholic.ac.kr (H. Koo).

¹ These authors contributed equally to this paper.

have loaded an actual drug onto the nanoparticle and transferred it to the inner ear to observe functional changes [5,6]. Drug delivery using polyethylene glycol-coated polylactic acid (PEG-PLA) nanoparticles has been attempted twice by the same group [6]. This group used cisplatin to deafen guinea pigs after systematical or intratympanic pretreatment with dexamethasone-loaded nanoparticles. In both studies, administration of dexamethasone-loaded nanoparticles protected hearing in the 4 kHz and 8 kHz frequencies. In another study, 6 α -methylprednisolone was loaded onto nanoparticles using alpha tocopherol derivatives, and cisplatin-induced hearing loss was protected at 10, 14, and 16 kHz [5]. These studies are meaningful in that they have observed actual changes in hearing through the delivery of drugs by nanoparticles. However, these studies lacked the information about proper surface properties of nanoparticles for inner drug delivery and also lacked the comparative study with the drugs used in clinic.

Unless we understand the key factors determining the distribution of nanoparticles in the inner ear, it may be impossible to develop useful drug carriers targeting the spiral ganglion and cochlear hair cells in efforts to recover hearing; it is essential to optimize the surface properties of nanoparticles. In our previous study, we synthesized nanoparticles based on poly(2-hydroxyethyl L-aspartamide) and octa-arginine, and co-delivered drugs and genes to the inner ear [7,8]. However, the safety and efficacy data remained inadequate. To explore further the correlations between the surface properties of nanoparticles and their distributions in the inner ear, we created four candidate nanoparticles based on phospholipid nanoemulsions. To compare the efficacies of inner ear drug delivery by particles differing in terms of charge [7], we constructed nanoparticles that were neutrally, negatively, and positively charged. We also attached polyethylene glycol (PEG) to positively charged nanoparticles in an effort to increase their circulation time in the perilymph (Scheme 1).

To screen the new nanoparticles, we developed a novel *in vitro* model quantitatively analyzing the extent of inner ear drug delivery. The inner ear is a tiny organ surrounded by the hardest bones of the body, and it is thus very difficult to analyze the levels of drugs delivered quantitatively. In many studies, drug concentrations in perilymph have been measured with the aid of high-performance liquid chromatography (HPLC). However, it is important to know the concentrations of drugs in the actual inner ear tissue, not the perilymph, because drugs can exert their effects only if absorbed into inner ear tissue from the perilymph. When a drug is delivered to the middle ear via intratympanic injection, that drug must pass through the round window membrane (RWM) or the annular ligament of the oval window (OW) to reach the inner ear. Although the precise mode of drug entry into the inner ear remains controversial, the RWM is now regarded as the dominant route [9]. The RWM consists of three layers, each about 70 μ m in thickness; drugs passing through the window become dispersed within the perilymph, which is similar in composition to cerebrospinal fluid, before finally being absorbed by inner ear tissue [10]. We reproduced this process *in vitro* using an artificial, viable, reconstructed, three-dimensional layer of human mucosa about 100 μ m thick; the level of a model drug delivered to cells at the bottom of culture plates was quantitatively measured via fluorescence-activated cell sorting (FACS; Fig. 3a).

To explore applications of nanoparticles *in vivo*, we loaded dexamethasone (Dex), currently used clinically to treat acute hearing loss, into nanoparticles selected by initial screening. Intratympanic steroid injection is a common salvage therapy for sudden hearing loss [11]. Next, we compared the biodistributions of Dex-loaded nanoparticles and their therapeutic efficacies, compared to those of Dex sodium phosphate (Dex-SP), in an animal model of ototoxicity. Conventionally, Dex is delivered as Dex-SP (a

hydrophilic salt) to increase drug solubility in water. However, we used Dex per se because hydrophobic drugs can be loaded into nanoparticle cores.

2. Materials and methods

2.1. Materials

1,2-Dipalmitoyl-*sn*-glycero-3-phosphocholine (DPPC) and 1,2-dipalmitoyl-*sn*-glycero-3-phosphoserine, sodium salt (DPPS) were purchased from Echelon Biosciences (Salt Lake City, UT). 1,2-Dipalmitoyl-*sn*-glycero-3-phosphoethanolamine-*N*-[methoxy-(polyethylene glycol)-2000] (DPPE-PEG2000) and 1,2-dipalmitoyl-3-trimethylammonium-propane (DPTAP) were purchased from Avanti Polar Lipids (Birmingham, AL). Flax seed oil and Nile Red were the products of Sigma-Aldrich (St. Louis, MO). Dex was purchased from Cayman Chemical (Ann Arbor, MI). Dexamethasone fluorescein (Dex-FITC) was purchased from Invitrogen (Carlsbad, CA). Dimethyl sulfoxide 99.0% (methyl sulfoxide, DMSO) and Triton X-100 were the products of Samchun Chemical (Seoul, South Korea). Phosphate-buffered saline (PBS, pH 7.4) was purchased from Gibco (Grand Island, NY). Dialysis Membrane (pre-wetted RC tubing, mol. wt. cut-off [MWCO]: 25 kDa) was purchased from Spectrum Laboratories (Rancho Dominguez, CA).

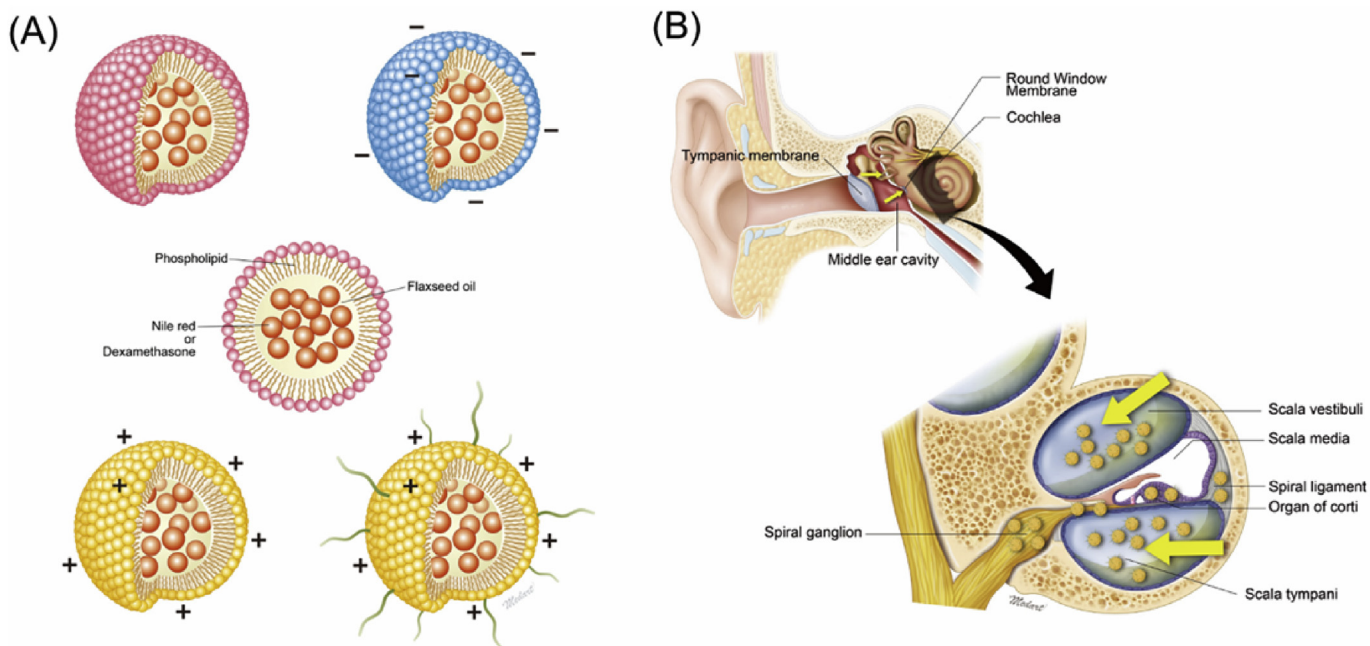
2.2. Nanoparticle preparation

Nanoparticles were prepared using a traditional O/W emulsion method in aqueous media employing DPPC only (6 mg), DPPC (2 mg)/DPPS (4 mg), DPPC (2 mg)/DPTAP (4 mg), and DPPE-PEG2000 (2 mg)/DPTAP (4 mg) to prepare neutral, anionic, cationic, and cationic-PEG nanoemulsions, respectively. Nile Red (0.3 mg) or Dex (10 mg) was dissolved in 20 μ L of DMSO, mixed with 50 mg of flax seed oil, and dispersed with the phospholipids by sonication in 2% (v/v) glycerol in water (lipid concentration: 2.4 mg/mL). Unloaded Nile Red and Dex were removed by dialysis (MWCO: 25 kDa) against distilled water for 1 h. The levels of Nile Red in nanoparticles were measured by fluorescence (510/605 nm) after complete liposome disruption with DMSO and Triton X-100.

The hydrodynamic radii and zeta potentials of all nanoparticles were measured at 25 $^{\circ}$ C in PBS (pH 7.2) with the aid of a Zetasizer (Nano ZS90; Malvern Instruments, Malvern, UK) running Data Transfer Support software. To evaluate nanoparticle morphology, negative staining was performed using a 2% (w/v) uranyl acetate solution followed by transmission electron microscopy. We used Dex-FITC to measure the loading efficacy and Dex release from nanoparticles. For release test, Dex:Dex-FITC 49:1 (w/w)-loaded nanoparticles were dialyzed against PBS (pH 7.2) at room temperature, and Dex-FITC fluorescence (485/530 nm) in PBS was measured over time. Because the saturation solubility of Dex in PBS at pH 7.4 is 90 μ g/ml, we used 1.0 L of the outer solution which is more than 10 folds of 100% drug release to make sink condition [12].

2.3. Screening of nanoparticle carriers

The cell uptake and cytotoxicity of nanoparticles were assessed using the immortalized mouse organ of Corti cell line HEI-OC1 kindly provided by Dr. M.K. Park (Seoul National University, College of Medicine, Seoul, South Korea). The establishment and characterization of the HEI-OC1 line have been described previously [13]. HEI-OC1 cells were grown and passaged in Dulbecco's Modified Eagle's Medium supplemented with 10% (v/v) fetal bovine serum and 50 U/mL recombinant mouse interferon- γ , in a humidified 10% (v/v) CO $_2$ environment at 33 $^{\circ}$ C.



Scheme 1. A schematic diagram of four candidate nanoparticles formed from phospholipid nanoemulsions (A), and the distributions of the nanoparticles after intratympanic administration (B).

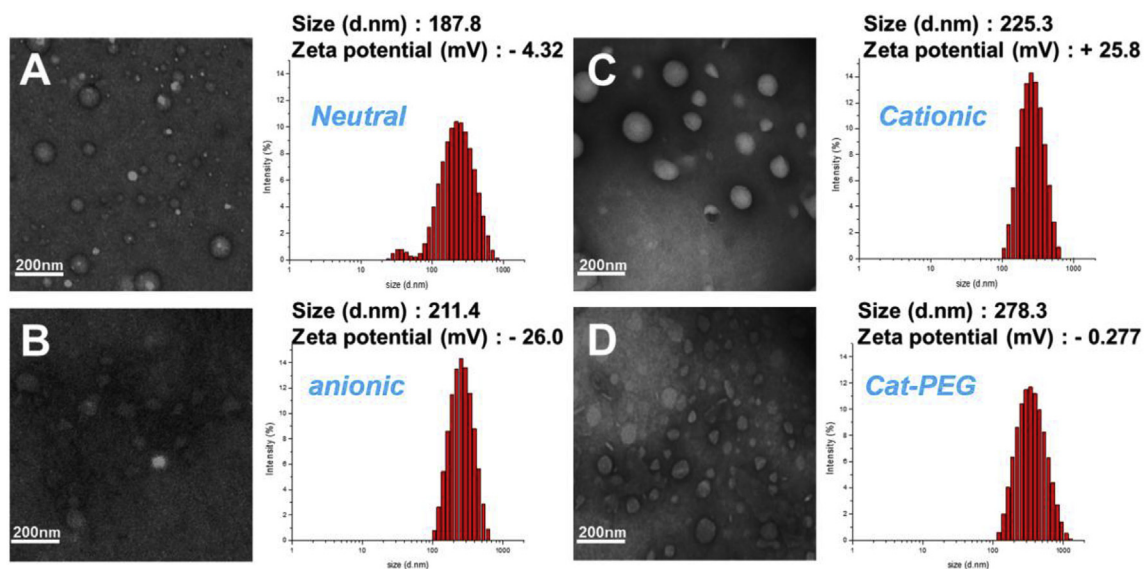


Fig. 1. The properties of nanoparticle carriers. The sizes and zeta potentials of nanoparticles were measured using a Zetasizer. The shapes were homogeneous as revealed by transmission electron microscopy.

The cytotoxicity of the four nanoparticles to HEI-OC1 cells were measured as follows. HEI-OC1 cells were plated in 96-well plates at 1×10^4 cells/well in 0.1 mL of complete growth medium and incubated to 80% confluence over 24 h. The cells were then incubated with the candidate nanoparticle carriers for 24 h. Cell viability was determined using the commercial MTT assay, in accordance with the manufacturer's protocol (EZ-Cytox; Daeil Lab, Seoul, South Korea). After incubation, optical densities were determined at 450 nm using a microplate reader (Bio-Rad Laboratories, Hercules, CA).

To measure cellular uptake of nanoparticles, HEI-OC1 cells were plated using the Lab-Tek™ II Chamber Slide™ System (Nunc, Roskilde, Denmark) and incubated with nanoparticle carriers

containing Nile Red for 4 h at the maximally safe doses as determined by cytotoxicity testing. Cells were fixed in 4% (v/v) paraformaldehyde, mounted using Vectashield Mounting Medium, stained with DAPI (Vector Laboratories, Burlingame, CA), and observed under a confocal microscope (LSM5 Live Configuration Variotwo VRGB; Zeiss, Jena, Germany) and via FACS (BD FACS Canto™ II; Becton Dickinson and Co., Franklin Lakes, NJ).

2.4. In vitro drug delivery to the inner ear using an artificial mucosa model

To mimic the RWM, we purchased a viable, reconstructed, three-dimensional, human mucosal layer (Neoderm®-OD; Tego

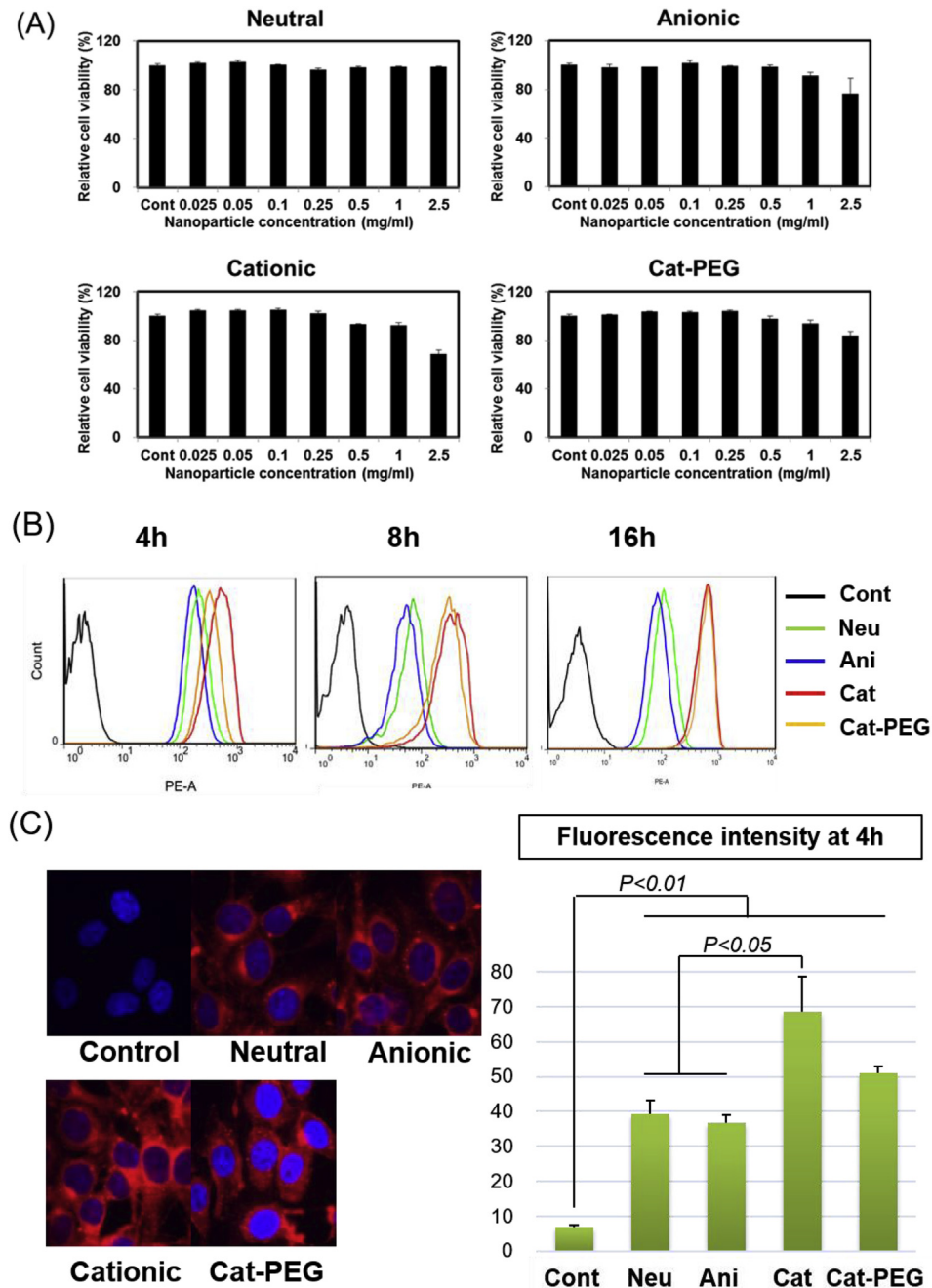


Fig. 2. The cytotoxicities and absorption rates of nanoparticle carriers. Cytotoxicity toward HEI-OC1 cells was evaluated using the MTT assay; the cells were exposed to various levels of nanoparticles. At 24 h, cationic nanoparticles were non-toxic up to 0.25 mg/mL, anionic and Cat-PEG nanoparticles were non-toxic up to 0.5 mg/mL, and neutral nanoparticles were non-toxic at all tested concentrations (a). Nanoparticle carrier uptake was observed using both FACS (b) and confocal microscopy after 4 h (c). Cationic nanoparticles afforded the most intense cellular uptake of Nile Red, followed by the Cat-PEG, neutral, and anionic nanoparticle carriers after 4 h (in that order). However, 16 h later, Cat-PEG nanoparticles showed uptake of nanoparticles similar to cationic nanoparticles in FACS data. All data shown are mean \pm SD of three independent experiments. p-values calculated by one-way ANOVA with Bonferroni posthoc test. Magnification \times 400.

Science, Seoul, South Korea). The epithelium is composed of human oral mucosal epithelial cells and the stroma of fibroblasts in a collagen matrix. The membrane is about 100 μ m thick, similar to the human RWM (about 70 μ m; [10]). The membrane was transferred to six-well plates containing monolayers of HEI-OC1 cells, and the plates were filled with cell culture medium that contacted the membrane (Fig. 3a). The four nanoparticle carriers loaded with Nile Red (1 μ g/mL) were applied to the membrane for 40 h, and dye uptake by cells was measured via confocal microscopy and FACS as described above.

2.5. Ex vivo cochlear tests

Primary cochlear explants were prepared from C57/BL6 mice at postnatal day 3 (P3). The dissected organs of Corti were incubated in high-glucose DMEM containing 5% (v/v) FBS, 5% (v/v) horse serum, and 10 ng/mL ampicillin at 37 $^{\circ}$ C under 5% (v/v) CO₂ in a humidified incubator. Nile Red-loaded nanoparticles at the maximum safe doses, and at half those doses, were added, and incubation proceeded for 24 h. After fixation in 4% (v/v) paraformaldehyde solution, permeabilization with acetone, antibody-

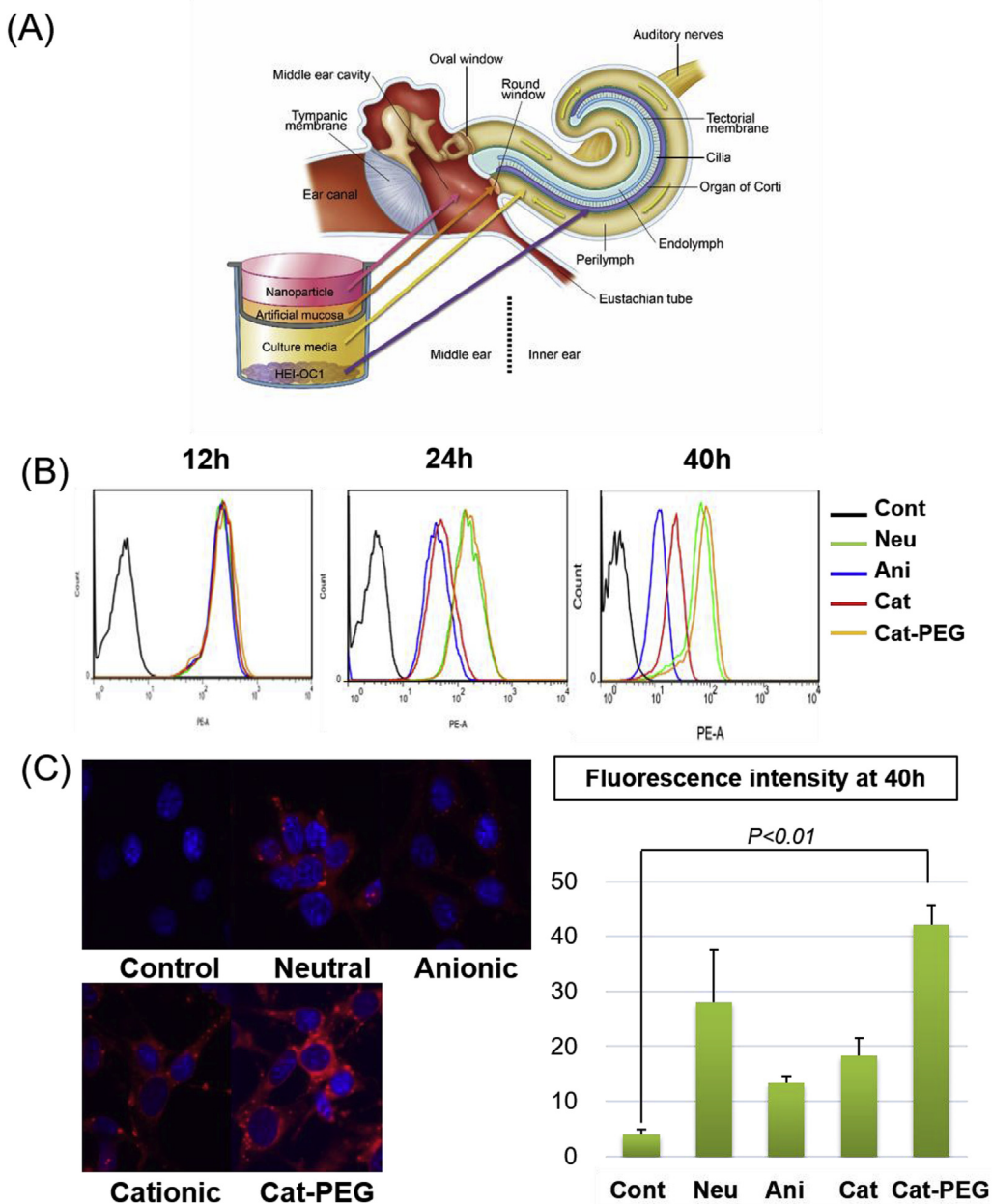


Fig. 3. A schematic diagram of our *in vitro* inner ear drug delivery model (a) and the results of FACS and confocal microscopy (b). The artificial mucosa, culture medium, and HEI-OC1 cells indicated at the bottom of the figure represent the round window membrane, perilymph, and hair cells, respectively (a). In FACS data, Cat-PEG nanoparticles and neutral nanoparticles showed the strongest fluorescence values, unlike the results of nanoparticle uptake without artificial mucosa (b). In the confocal microscopy results, the difference in fluorescence intensities between nanoparticles were not statistically significant, and only Cat-PEG nanoparticles were significantly different from the control group. All data shown are mean \pm SD of three independent experiments. p-values calculated by one-way ANOVA with Bonferroni posthoc test. Magnification $\times 400$.

binding using Alexa Fluor 488 Phalloidin (Molecular Probes, Eugene, OR), and mounting in Vectashield Mounting Medium containing DAPI (Vector Laboratories), nanoparticle uptakes were measured by fluorescence microscopy (Eclipse TE300 Microscope; Nikon, Tokyo, Japan; low magnification) and confocal microscopy (high magnification). All specimens were stained with DAPI and FITC-labeled phalloidin to evaluate the status of hair cell cilia and tissue architecture.

2.6. Surgery

The surgical procedure for 1-month-old male C57/BL6 mice has

been described previously [7]. Before surgery, the mice were anesthetized with a mixture of 30 mg/kg Zoletil (Virbac, Carros, France) and 10 mg/kg Rompun (Bayer, Leverkusen, Germany), placed on a thermoregulated heat pad in the supine position, a midline incision was made, and the left-side bulla was exposed. A bullar hole was created using fine forceps. Next, Dex-loaded nanoparticles at the maximum safe dose (nanoparticle concentration 0.5 mg/mL, Dex concentration 0.14 mg/mL) or Dex-SP (5 mg/mL) was injected into the middle ear cavity until the cavity was full. To reflect the clinical situation, we did not use gel foam to retain the drug in the middle ear. The hole was blocked with bone wax (B. Braun, Melsungen, Germany) and the wound was closed. After

operation, Rimadyl (1.0 mg/kg; Pfizer, Walton Oaks, UK) was injected to relieve pain. Baytril (10 mg/kg; Orion, Hamburg, Germany) was intraperitoneally injected once daily as prophylaxis against middle ear infection.

2.7. *In vivo* nanoparticle screening

Four kinds of nanoparticle carriers containing Nile Red were injected into the middle ear cavity by the method described above. At 24 h after operation, mice were sacrificed and the cochleae were harvested. They were then rinsed with tap water for 1 min to remove outer surface particles, stored in 4% (v/v) paraformaldehyde (Merck, Darmstadt, Germany) for 20 min, rinsed with PBS, and the area of the auditory epithelium and spiral limbus were dissected for whole-mount preparations. After mounting using Vectashield Mounting Medium, stained with DAPI (Vector Laboratories, Burlingame, CA), and nanoparticle uptakes were observed under a confocal microscope (LSM5 Live Configuration Variotwo VRGB; Zeiss, Jena, Germany).

2.8. *In vivo* drug distributions

At 1, 24, and 72 h after operation, mice were sacrificed and the cochleae were harvested. They were then rinsed with tap water for 1 min to remove outer surface particles, stored in 4% (v/v) paraformaldehyde (Merck, Darmstadt, Germany) for 24 h, fixed overnight, decalcified with 5% (w/v) EDTA (0.3 M, pH 6.5), and embedded in paraffin as described elsewhere [14]. Midmodiolar 5- μ m-thick sections were obtained and stained using the Vectastain Elite ABC HRP Kit and the Vector NovaRED Peroxidase Substrate (Vector Laboratories, Burlingame, CA). The sections were also stained with an anti-Dex antibody as directed by the manufacturer (Abcam, UK) to detect Dex and Dex-SP.

2.9. A mouse model of ototoxicity

One-month-old male C57/BL6 mice were divided into four groups. The control group received no surgery or treatment, and the other three groups received middle ear drugs 2 h prior to the induction of ototoxicity, as described below; these groups then received nanoparticle-loaded Dex, Dex-SP, or saline (sham group). Ototoxicity was induced by the subcutaneous injection of kanamycin (500 mg/kg; Sigma-Aldrich, St. Louis, MO) and the intraperitoneal injection of furosemide (120 mg/kg; Sigma-Aldrich) 30 min later. Forty hours later, some mice were sacrificed for RT-PCR and the remaining mice were subjected to ABR testing and whole-mount staining of the organ of Corti 1 week later.

2.10. ABR test *in vivo*

ABR responses were evoked 7 days after the induction of ototoxicity using a System III Evoked Potential Workstation (Tucker-Davis Technologies, Alachua, FL). Briefly, mice were anesthetized with a mixture of 30 mg/kg Zoletil (Virbac, Carros, France) and 10 mg/kg Rompun (Bayer, Leverkusen, Germany) and each animal was placed on a heating pad inside a soundproof acoustic chamber. For ABR testing, click and tone burst stimuli (4, 8, 16, and 32 kHz) were presented by an MF1 magnetic speaker (Tucker-Davis Technologies, Alachua, FL) from 90 to 20 dB SPL in 5–10 dB SPL steps [15]. The click stimuli were 0.1 ms in duration and the tone burst stimuli were 5 ms in duration (2.5 ms each for rise and decay, thus without a plateau). Threshold responses were defined as the sound pressure levels at which the peak amplitudes of the evoked responses (latency, 2.5–7.5 ms) were greater than two standard deviations above the average background activity prior to stimulus

onset (over 15–20 ms). Threshold differences among mouse groups were statistically compared. After ABR measurement, all mice were sacrificed for cochlear whole mounting.

2.11. RT-PCR of cochlear samples

Total cochlear RNA was extracted using an easy-BLUE Total RNA Extraction kit (iNtRON Biotechnology, Seongnam, South Korea). cDNA was synthesized using a Reverse Transcriptase Premix kit (Elpis Biotech, Daejeon, South Korea) and amplified employing a Power SYBR™ Green Polymerase Chain Reaction (PCR) Master Mix (Applied Biosystems, Foster City, CA) using gene-specific primer pairs: IL1 β -forward, 5'-GCC CAT CCT CTG TGA CTC AT-3', IL1 β -reverse, 5'-AGG CCA CAG GTA TTT TGT CG-3'; IL6-forward, 5'-CCG GAG AGG AGA CTT CAC AG-3', IL6-reverse, 5'-CCG GAG AGG AGA CTT CAC AG-3'; TNF α -forward, 5'-ACG GCA TGG ATC TCA AAG AC-3', TNF α -reverse, 5'-GTG GGT GAG GAG CAC GTA GT-3'; and IFN γ -forward, 5'-GCT ACA CAC TGC ATC TTG GCT TT-3', IFN γ -reverse, 5'-AAT GAC TGT GCC GTG GCA GTA A-3'. Quantitative real-time PCR was performed using ABI 7500 FAST (Applied Biosystems). The expression levels of mRNAs were normalized to that encoding glyceraldehyde-3-phosphate dehydrogenase (GAPDH). The $\Delta\Delta$ Ct method was used for data analysis with the aid of a Microsoft Excel spreadsheet containing algorithms provided by the manufacturer. Fold changes were calculated and expressed as log-normalized ratios compared with the values of the saline-treated group.

2.12. Whole mounting of the organ of Corti (OC)

After ABR measurements, mice were sacrificed and the cochleae were collected, fixed, and decalcified as described above. Using a sharp-angled micro-scalpel, the bony and membranous labyrinths and the tectorial membrane were carefully removed to expose the organ of Corti (OC), which was sectioned into two portions, one containing the apex and the middle cochlear turn and the other the basal cochlear turn. The samples were placed into Nunclon Microwell Plates (Sigma-Aldrich) filled with PBS and stored at 4 °C. Later, the samples were permeabilized with 0.5% (v/v) Triton X-100 (Sigma-Aldrich) for 15 min at room temperature with shaking and incubated for 1 h with a 1:1000 dilution of phalloidin (R Alexa Fluor 488, Invitrogen, Carlsbad, CA) in PBS. After three washes in PBS, the samples were transferred to slides, mounted with the aid of Vectashield mounting medium, and stained with DAPI (Vector Laboratories) [16].

2.13. Analysis of images

The fluorescence intensities of the photographs obtained using the confocal microscope were analyzed using the confocal microscope company's software, ZEN blue (Zeiss, Jena, Germany). Immunofluorescence signal from the light microscope was analyzed and quantified using ImageJ. The photographs obtained from three independent experiments were analyzed, and for cell images, 10 cells were randomly selected from each photograph were analyzed.

2.14. Statistical analysis

All data are presented as means \pm standard errors of measurements performed in triplicate. Statistical significance was tested using one-way analysis of variance (ANOVA) with Bonferroni post-test was used for to explore differences among several group at all results except ABR comparison. Kruskal-Wallis test with Holm–Bonferroni post-test was used for ABR comparison. In all analyses, a p-value <0.05 was taken to indicate statistical

significance.

2.15. Study approval

All procedures were performed in accordance with national ethics guidelines. This study was approved by the Institutional Review Board of our hospital (approval no. CMCDJ-AP-2016-011).

3. Results

3.1. Preparation and characterization of nanoparticles

Nanoparticles were prepared using traditional oil-in-water emulsion method based on self-assembly. The cores were filled with flax seed oil and the shells were composed of different phospholipids. Nile Red and Dex were loaded into the cores. The nanoparticles were about 200 nm in diameter, and transmission electron microscopy (TEM) revealed that all were spherical under aqueous conditions (Fig. 1). Due to the use of DPTAP with cationic charge and DPPS with anionic charge, the zeta potentials were -4.32 , -26.0 , $+25.8$, and -0.28 , respectively, for neutral, anionic, cationic, and cationic-PEG nanoparticles. Thus, the surface charges were controlled by varying the phospholipids, but the nanoparticle diameters were not affected much by this. We observed the size of the nanoparticles for one week, and neutral, anionic and Cat-PEG particles were stable in PBS at pH 7.4 (Supplementary data 1). However, cationic nanoparticles showed large aggregation from 1 day. The exact reason of aggregation could not be determined and will be studied in future studies.

3.2. Screening of candidate nanoparticle carriers

The toxicities of nanoparticles to cells were measured using the commercial 3-(4,5-dimethylthiazol-2-yl)-2,5-diphenyltetrazolium bromide (MTT) assay. The levels at which nanoparticles did not affect cell viability (compared with untreated cells) were 0.5 mg/mL for anionic, 0.25 mg/mL for cationic, and 0.5 mg/mL for Cat-PEG nanoparticles. Neutral nanoparticles were not toxic up to 2.5 mg/mL (Fig. 2a). The cellular uptakes of Nile Red-loaded nanoparticles

by HEI-OC1 cells were tested under conventional culture conditions. Cells were treated with 0.5 mg/mL of each kind of nanoparticle, and then subjected to FACS and confocal microscopy. Cationic nanoparticles afforded the most intense cellular uptake of Nile Red, followed by the Cat-PEG, neutral, and anionic nanoparticle carriers after 4 h (in that order). However, 16 h later, Cat-PEG nanoparticles showed uptake of nanoparticles similar to cationic nanoparticles in FACS data (Fig. 2b and c).

We used our *in vitro* inner ear RWM model to measure the intensity of Nile Red fluorescence in HEI-OC1 cells after the delivery of nanoparticles from culture medium through an artificial mucosal membrane. In FACS data, Cat-PEG nanoparticles and neutral nanoparticles showed the strongest fluorescence values, unlike the results of nanoparticle uptake without artificial mucosa (Fig. 3b). Interestingly, the uptake efficacy of neutral nanoparticles was comparable to that of Cat-PEG nanoparticles. In the comparison of absorption of four nanoparticles by organotypic cultures, absorption of Nile Red was significantly stronger in cationic nanoparticle among the four nanoparticles, followed by Cat-PEG nanoparticle, and these results were similar to the *in vitro* results in the absence of artificial mucosa (Supplementary data 2).

For the *in vivo* screening of four nanoparticles, we observed the intensity of Nile red fluorescence in the organ of Corti with a confocal microscope, 24 h after administrating the four nanoparticles loading Nile red in the middle ear cavity. Fluorescence intensity in the organ of Corti was significantly higher in Cat-PEG nanoparticles compared to other nanoparticles, and the other three particles did not show significant fluorescence intensity compared to the control (Fig. 5). Thus, Cat-PEG nanoparticles were chosen for further study.

3.3. Ex vivo and in vivo drug delivery to the inner ear using Cat-PEG nanoparticles

Isolated organs of Corti were treated with a safe level of Cat-PEG nanoparticles. We measured Nile Red uptake in organotypic cultures, and monitored the cilia of hair cells and the micro-architecture of the organ of Corti. Neither the hair cells nor the organ of Corti were damaged in any way after 24 h of exposure to

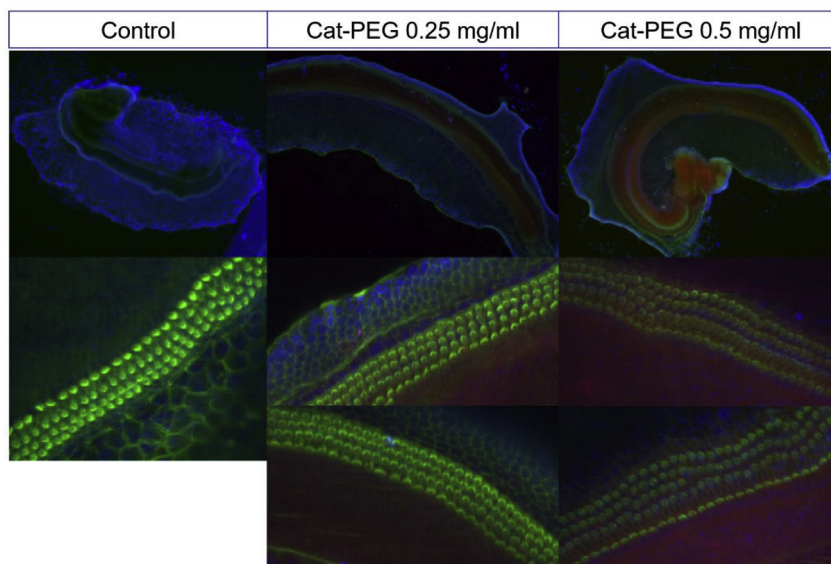


Fig. 4. Absorption of Cat-PEG nanoparticles by organotypic cultures to 24 h of treatment. The cilia of hair cells and the architecture of the organ of Corti remained undamaged to 24 h; Nile Red was absorbed to a greater extent by the 0.5 mg/mL than by the 0.25 mg/mL group. Both groups exhibited high-level absorption of Nile Red on the medial sides of the organotypic cultures. Magnifications 40 \times (fluorescent microscopy) and 200 \times (confocal microscopy).

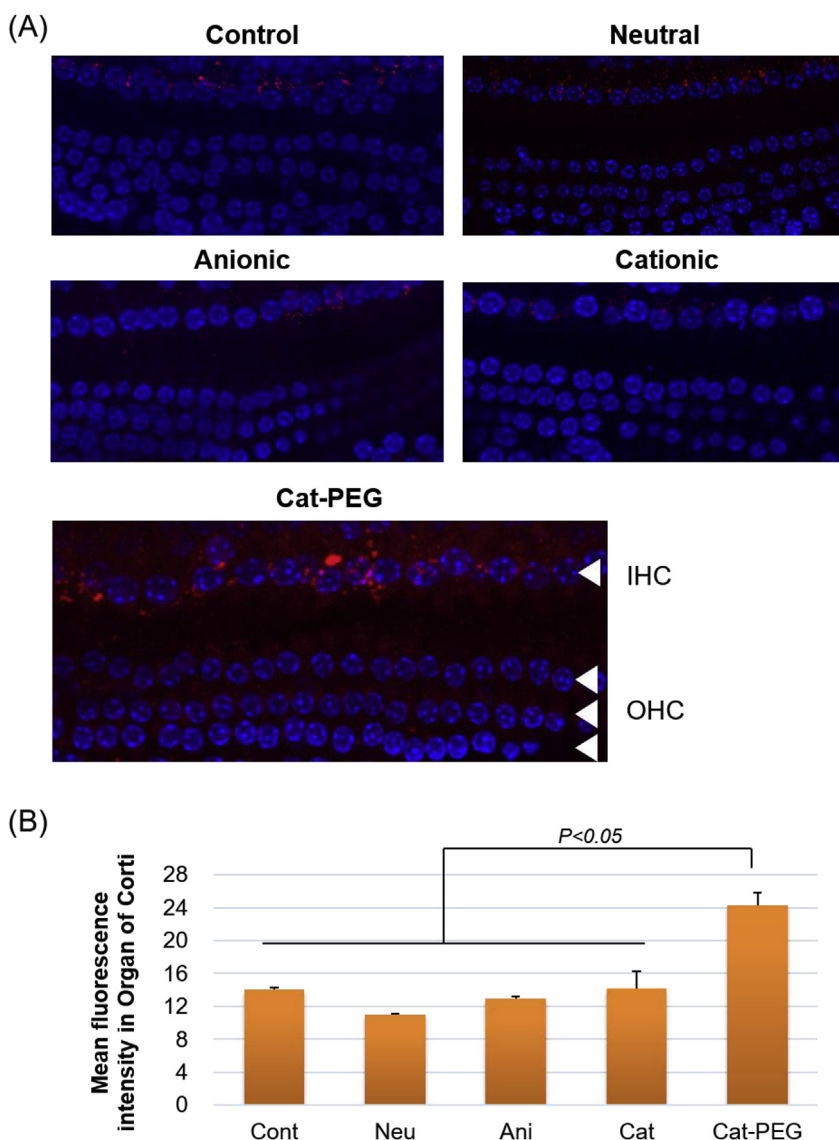


Fig. 5. *In vivo* screening results of four nanoparticles and confocal microscopy images of organ of Corti. The cochleae were sampled 24 h after administering the four nanoparticles loading Nile Red in the middle ear cavity. The intensity of the Nile Red fluorescence absorbed in the organ of Corti was compared with confocal microscope. Although some autofluorescence was observed in all samples in inner hair cells, fluorescence intensity of whole organ of Corti was statistically significantly higher in Cat-PEG nanoparticles.

either 0.25 or 0.5 mg/mL Cat-PEG nanoparticles; more Nile Red was absorbed by the 0.5 mg/mL than by the 0.25 mg/mL group. Nile Red was strongly absorbed on the medial sides of the organotypic cultures (the spiral ganglia and lamina; Fig. 4).

We next loaded Dex into Cat-PEG nanoparticles. The loading efficacy was $93.1 \pm 7.6\%$ and the particle diameter was about 143.53 ± 21.18 nm, similar to that before drug loading. Dex was slowly released from all four nanoparticles suspended in PBS (pH 7.4) (Supplementary data 3). About half of the Dex was released after 24 h, and the release rate became slower after that (Supplementary data 3). After injection of Cat-PEG-Dex or Dex-SP into the middle ear cavity, we immunohistochemically explored drug distributions using an antibody targeting Dex and Dex-SP. As shown in Fig. 6, both groups exhibited strong absorption of Dex or Dex-SP by inner ear tissue from 1 to 24 h after drug administration, especially by the medial portion of the cochlea including the modiolus, spiral ganglion, and spiral lamina (where absorption was stronger than that by the outer capsule or lateral wall). The Cat-PEG-Dex group absorbed slightly more Dex than the Dex-SP

group, but the difference was not significant. Seventy-two hours after administration, weak Dex or Dex-SP uptake remained evident in the spiral ganglia and inner hair cells of the cochleae of both groups (Fig. 6).

3.4. Therapeutic effects of Cat-PEG-Dex and Dex-SP in a mouse model of ototoxicity

The auditory brainstem response (ABR) thresholds of the three groups were measured on day 7, and the Kruskal-Wallis test revealed significant among-group differences at 4 kHz ($p = 0.001$), 8 kHz ($p = 0.002$), 16 kHz ($p = 0.002$), 32 kHz ($p < 0.001$), and in the click test ($p = 0.001$) (Fig. 7a). Upon post hoc testing using the Holm–Bonferroni method, the Deaf-Cat-PEG-Dex group exhibited significantly better hearing than the Deaf-Dex-SP group at 4 kHz ($p = 0.008$), 8 kHz ($p = 0.008$), 16 kHz ($p = 0.008$), 32 kHz ($p = 0.005$), and in the click test ($p = 0.008$); and also better hearing than the Deaf-saline group at 4 kHz ($p = 0.012$), 8 kHz ($p = 0.012$), 16 kHz ($p = 0.012$), 32 kHz ($p = 0.010$), and in the click test

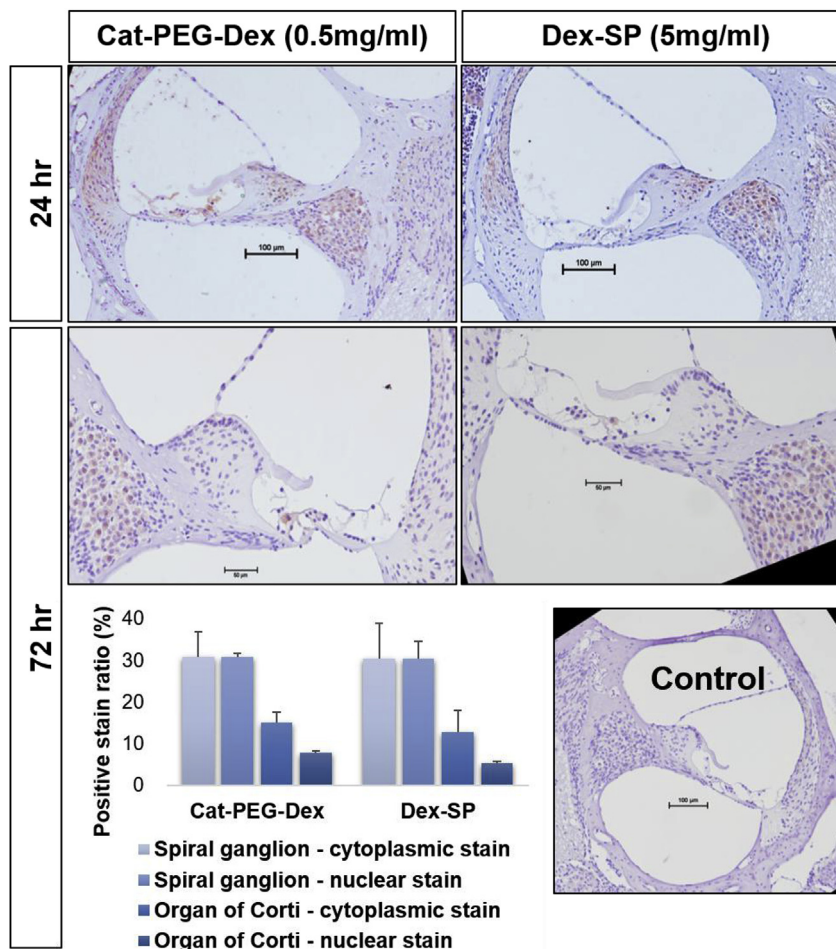


Fig. 6. Immunostaining for dexamethasone (Dex) or dexamethasone sodium phosphate (Dex-SP) after injection of Cat-PEG-Dex or Dex-SP into the middle ear cavity. Both groups exhibited strong absorption of Dex or Dex-SP by inner ear tissue from 1 to 24 h after administration, especially in the medial portion of the cochlea. At 72 h after administration, weak Dex or Dex-SP uptake remained evident in the spiral ganglions and inner hair cells of the cochleae of both groups and positive staining ratio between the two groups was not statistically different.

($p = 0.012$). However, no significant difference was observed between the Deaf-Saline and Deaf-Dex-SP groups at any frequency.

We then triggered an antibiotic-induced inflammatory reaction, as revealed by quantitative PCR. The expression levels of the pro-inflammatory cytokines IFN- γ , IL-6, IL-12, and IL-1- β were upregulated by the antibiotic, and this process was inhibited by Dex-SP but more so by Cat-PEG-Dex (Fig. 7b). To explore the protective effects afforded by Cat-PEG-Dex or Dex-SP against kanamycin and furosemide, whole-mounted organs of Corti stained with phalloidin were observed by confocal microscopy, focusing on four specific regions of the place-frequency map [17]. As shown in Fig. 7c, the Deaf-Saline group exhibited severe loss of stereocilia and hair cells in all four frequency regions; the Deaf-Cat-PEG-Dex group exhibited some damage at the 16 kHz site but the tissues were otherwise as well preserved as those of the control group. The extent of damage in the Deaf-Dex-SP group was intermediate between those of the Deaf-saline and the Deaf-Cat-PEG-Dex groups.

4. Discussion

We earlier reported that positively charged particles were predominantly absorbed by HEI-OC1 cells (*in vitro*) and organotypic cultures of the organ of Corti (*ex vivo*; 7). However, if drug delivery to hair cells *in vivo* is to be successful, a crucial question remains.

Can the drug pass through the RWM to become dissolved in the aqueous perilymph and ultimately absorbed by inner ear cells? It remained unclear whether positively charged particles would be better in this context than particles with neutral or negative charges. We developed an *in vitro* model system to answer this question. As mentioned above, it was also essential to measure the level of drug absorbed by inner ear tissue per se, not just the drug concentration in perilymph.

In previous experiments, semi-permeable membranes or actual animal RWMs have been used as *in vitro* or *ex vivo* RWM models [18–20]. Little is known about the individual aspects of transmembrane transport involved in substance absorption through the RWM; these may include passive and/or carrier-facilitated diffusion, active transport, and/or phagocytosis [21]. These methods modulate drug diffusion through the membrane, but not drug interactions with living cells of the RWM. Recently, a model featuring Madin-Darby canine kidney (MDCK) epithelial cells deposited on a porcine, small intestinal, submucosal collagen matrix has been described, which partially overcomes the disadvantages of the previous model [22,23]. However, the cited authors described only permeation of the artificial RWM, not drug dispersion in perilymph or drug absorption by inner ear cells. Here, we used a human mucosal, cell-based artificial mucosa to model inner ear drug delivery. Notably, the results differed from those obtained when drug

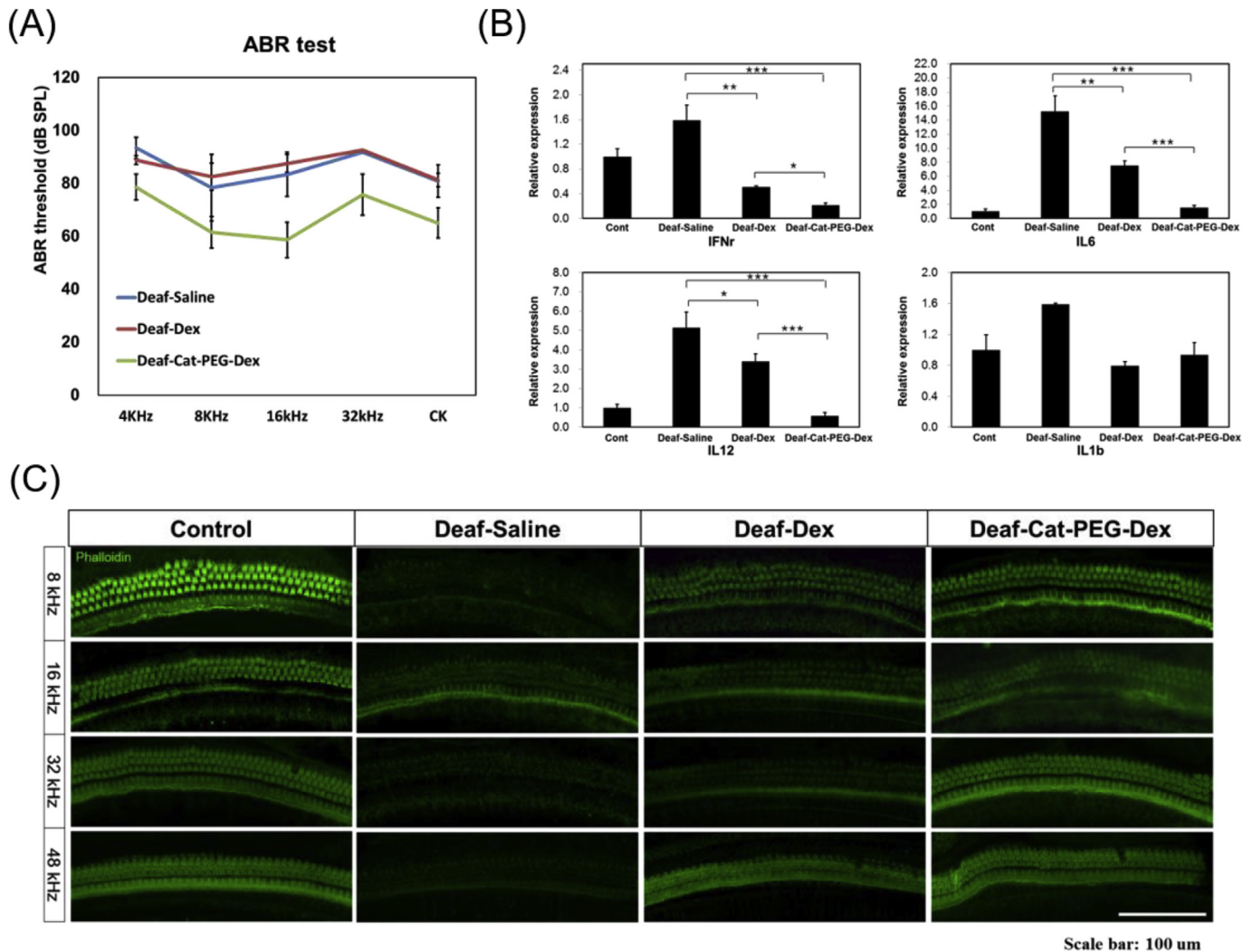


Fig. 7. Therapeutic outcomes afforded by Cat-PEG-Dex in a mouse model of ototoxicity. The ABR thresholds of the three groups ($n = 6/\text{group}$) were measured on day 7; the Deaf-Cat-PEG-Dex group exhibited significantly better hearing than the Deaf-Dex-SP and Deaf-saline groups at all frequencies tested. The statistical results are shown in the text. (a). In terms of the expression levels of pro-inflammatory cytokines 40 h after the induction of deafness, inhibition thereof was evident in the Dex-SP group but more prominently in the CAT-PEG-Dex group. The data represent the means \pm S.D. from three independent experiments performed in duplicate. * denotes $P < 0.05$, ** denotes $P < 0.01$, and *** denotes $P < 0.001$ (b). The whole-mount organs of Corti of the Deaf-saline group exhibited severe loss of stereocilia and hair cells in all four frequency regions; although the Deaf-Cat-PEG-Dex group exhibited some damage at the 16-kHz site, the other sites were as well preserved as those of the control group (c).

uptake by HEI-OC1 monolayers in culture dishes was evaluated. We found that Cat-PEG or neutral particles facilitated inner ear drug delivery.

However, unlike the results of the screening of nanoparticles using artificial mucosa, the screening of the delivery of nanoparticles *in vivo* revealed that only Cat-PEG nanoparticles were significantly transferred to the organ of Corti. This may be due to that our artificial mucosa model was not perfect and has limitations in reproducing the three-dimensional structure of inner ear tissues, or a circulation of perilymph in cochlea. Cat-PEG nanoparticles were found to be superior in both *in vitro* artificial mucosa screening and *in vivo* screening. Therefore, based on multiple screening experiments, our results pointed out the importance of PEG on the nanoparticle surface for inner ear drug delivery system as well as for other situation including intravenous injection of nanoparticles.

It is well known that positively charged particles exhibit good cellular uptake because they easily bind to cell surface glycoproteins with negative charges [24]. We found as much when

evaluating uptake by HEI-OC1 monolayers in culture dishes. However, this did not mean that such particles would be superior in terms of mucosal permeation. We considered that cationic particles might not readily exit the mucosa because they might become attached to cells or the extracellular matrix. PEG coating has traditionally been used to prevent nanoparticle aggregation and unintended interactions with molecules such as serum proteins [25]. Hanes reported that PEG-coated nanoparticles diffused >100-fold more rapidly than did particles lacking PEG [26]. We thus hypothesized that coating nanoparticles with PEG would improve the extent of inner ear delivery. We found that cationic charges inhibited nanoparticle penetration in the inner ear RWM model, although cellular uptake was enhanced; we thought that PEG might overcome this limitation.

Our nanoparticles can carry hydrophobic drugs in their hydrophobic cores; we used Dex in the present experiments. It was previously reported that conversion of Dex-SP to Dex was slower than expected when Dex-SP was injected into the middle ear; the perilymph concentrations of Dex and Dex-SP were simultaneously

measured by HPLC [27]. We delivered active Dex (not Dex-SP) in nanoparticles at 0.14 mg/mL, thus >30-fold lower than the Dex-SP level. However, the extents of Dex and Dex-SP absorption by the inner ear *in vivo* were similar, and Dex afforded better anti-inflammatory action and hearing protection in an animal model of ototoxicity. Although we did not measure drug concentrations in perilymph, Dex-SP was better dispersed in perilymph than were nanoparticles containing Dex, attributable to the low molecular weight of Dex-SP, in line with the results of earlier experiments on the influence of particle size on the extent of RWM permeation [28]. Therefore, the better anti-inflammatory action and hearing protection afforded by nanoparticles may reflect extensive loss of Dex-SP during delivery to target cells after injection, or lower cellular uptake and an ineffective therapeutic effect of DEX-SP attributable to incomplete conversion to DEX. After systemic administration, Dex-SP circulates in the blood and much may be converted into the active form of the drug prior to attainment of the target tissue. Therefore, for many hydrophobic drugs, administration as salts affords good results and excellent cost-effectiveness. However, in terms of local drug delivery to tissues such as the inner ear, where drugs are absorbed and discharged rapidly, we found that a nanoparticle formulation of the active drug was much more effective than the salt form.

5. Conclusion

In summary, we developed an *in vitro* RWM model to screen nanoparticles, and optimized the surface properties thereof in terms of inner ear drug delivery. We successfully delivered Dex to inner ear hair cells with the aid of Cat-PEG nanoparticles, obtaining better therapeutic results than afforded by Dex-SP in an animal model of ototoxicity. Additional testing of drug safety is required, and the optimal drug combinations for nanoparticle loading must be further explored.

Data availability

All the data needed to reproduce the work performed and evaluate the conclusions made are presented in the paper and/or the Supplemental Materials. Additional raw/processed data forms part of an ongoing study and may be requested from the authors.

Acknowledgments

We thank the Chung-cheong Otolaryngology Moyim for their assistance with audiological testing, statistical advice, and help with the whole-mount experiments; and Prof. Insung S. Choi (KAIST) for suggesting the creation of an *in vitro* model of the inner ear RW. This research was supported by the Basic Science Research Program of the National Research Foundation of Korea (NRF) funded by the Ministry of Education (grant nos. NRF-2017R1D1A1B03027894 and 2016R1C1B3013951); the Catholic University of Korea Daejeon St. Mary's Hospital; and a Clinical Research Institute Grant from the Catholic University of Korea Daejeon St. Mary's Hospital (grant no. CMCDJ-P-2017-001).

Appendix A. Supplementary data

Supplementary data related to this article can be found at <https://doi.org/10.1016/j.biomaterials.2018.04.038>.

References

- [1] S.K. Juhn, L.P. Rybak, W.L. Fowlks, Transport characteristics of the blood–perilymph barrier, *Am. J. Otolaryngol.* 3 (1982) 392–396.
- [2] H. Sajjadi, M.M. Paparella, Meniere's disease, *Lancet* 372 (2008) 406–414.
- [3] W.H. Slaterry, L.M. Fisher, Z. Iqbal, R.A. Friedman, N. Liu, Intratympanic steroid injection for treatment of idiopathic sudden hearing loss, *Otolaryngol. Head Neck Surg. Off. J. Am. Acad. Otolaryngol. Head Neck Surg.* 133 (2005) 251–259.
- [4] I. Pyykko, J. Zou, W. Zhang, Y. Zhang, Nanoparticle-based delivery for the treatment of inner ear disorders, *Curr. Opin. Otolaryngol. Head Neck Surg.* 19 (2011) 388–396.
- [5] S. Martin-Saldana, R. Palao-Suay, A. Trinidad, M.R. Aguilar, R. Ramirez-Camacho, J. San Roman, Otoprotective properties of 6alpha-methylprednisolone-loaded nanoparticles against cisplatin: *in vitro* and *in vivo* correlation, *Nanomed. Nanotechnol. Biol. Med.* 12 (2016) 965–976.
- [6] C. Sun, X. Wang, D. Chen, X. Lin, D. Yu, H. Wu, Dexamethasone loaded nanoparticles exert protective effects against Cisplatin-induced hearing loss by systemic administration, *Neurosci. Lett.* 619 (2016) 142–148.
- [7] J.Y. Yoon, K.J. Yang, D.E. Kim, K.Y. Lee, S.N. Park, D.K. Kim, et al., Intratympanic delivery of oligoarginine-conjugated nanoparticles as a gene (or drug) Carrier to the inner ear, *Biomaterials* 73 (2015) 243–253.
- [8] D.K. Kim, S.N. Park, K.H. Park, C.W. Park, K.J. Yang, J.D. Kim, et al., Development of a drug delivery system for the inner ear using poly(amino acid)-based nanoparticles, *Drug Deliv.* 22 (2015) 367–374.
- [9] A.N. Salt, E.B. King, J.J. Hartsock, R.M. Gill, S.J. O'Leary, Marker entry into vestibular perilymph via the stapes following applications to the round window niche of Guinea pigs, *Hear. Res.* 283 (2012) 14–23.
- [10] S. Yoda, S. Cureoglu, S. Shimizu, N. Morita, H. Fukushima, T. Sato, et al., Round window membrane in Meniere's disease: a human temporal bone study, *Otol. Neurotol. : Off. Publ. Am. Otol. Soc. Am. Neurotol. Soc. Eur. Acad. Otol. Neurotol.* 32 (2011) 147–151.
- [11] R.J. Stachler, S.S. Chandrasekhar, S.M. Archer, R.M. Rosenfeld, S.R. Schwartz, D.M. Barrs, et al., Clinical practice guideline: sudden hearing loss, *Otolaryngol. Head Neck Surg. Off. J. Am. Acad. Otolaryngol. Head Neck Surg.* 146 (2012) S1–S35.
- [12] B. Balzus, M. Colombo, F.F. Sahle, G. Zoubari, S. Staufienbiel, R. Bodmeier, Comparison of different *in vitro* release methods used to investigate nanocarriers intended for dermal application, *Int. J. Pharm.* 513 (2016) 247–254.
- [13] G.M. Kalinec, P. Webster, D.J. Lim, F. Kalinec, A cochlear cell line as an *in vitro* system for drug ototoxicity screening, *Audiol. Neuro. Otol.* 8 (2003) 177–189.
- [14] R. Riquelme, R. Cediell, J. Contreras, R.D. la Rosa Lourdes, S. Murillo-Cuesta, C. Hernandez-Sanchez, et al., A comparative study of age-related hearing loss in wild type and insulin-like growth factor I deficient mice, *Front. Neuroanat.* 4 (2010) 27.
- [15] R. Cediell, R. Riquelme, J. Contreras, A. Diaz, I. Varela-Nieto, Sensorineural hearing loss in insulin-like growth factor I-null mice: a new model of human deafness, *Eur. J. Neurosci.* 23 (2006) 587–590.
- [16] L. Sanz, S. Murillo-Cuesta, P. Cobo, R. Cediell-Algovia, J. Contreras, T. Rivera, et al., Swept-sine noise-induced damage as a hearing loss model for preclinical assays, *Front. Aging Neurosci.* 7 (2015) 7.
- [17] A. Viberg, B. Canlon, The guide to plotting a cochleogram, *Hear. Res.* 197 (2004) 1–10.
- [18] A.A. Aarnisalo, P. Aarnisalo, L. Pietola, J. Wahlfors, J. Jero, Efficacy of gene transfer through the round window membrane: an *in vitro* model, *ORL J. Oto-Rhino-Laryngol. its Relat. Specialties* 68 (2006) 220–227.
- [19] S.H. Park, I.S. Moon, Round window membrane vibration may increase the effect of intratympanic dexamethasone injection, *Laryngoscope* 124 (2014) 1444–1451.
- [20] J.M. Wazen, J.P. Stevens, H. Watanabe, J.W. Kysar, A.K. Lalwani, Silver/silver chloride microneedles can detect penetration through the round window membrane, *J. Biomed. Mater. Res. Part B Appl. Biomater.* 105 (2017) 307–311.
- [21] A.N. Salt, S.K. Plontke, Principles of local drug delivery to the inner ear, *Audiol. Neuro. Otol.* 14 (2009) 350–360.
- [22] X. Du, K. Chen, S. Kuriyavar, R.D. Kopke, B.P. Grady, D.H. Bourne, et al., Magnetic targeted delivery of dexamethasone acetate across the round window membrane in Guinea pigs, *Otol. Neurotol. Off. Publ. Am. Otol. Soc. Am. Neurotol. Soc. Eur. Acad. Otol. Neurotol.* 34 (2013) 41–47.
- [23] F.G. Mondalek, Y.Y. Zhang, B. Kropp, R.D. Kopke, X. Ge, R.L. Jackson, et al., The permeability of SPION over an artificial three-layer membrane is enhanced by external magnetic field, *J. Nanobiotechnol.* 4 (2006) 4.
- [24] S. Lee, S.-Y. Lee, S. Park, J.H. Ryu, J.H. Na, H. Koo, et al., *In vivo* NIRF imaging of tumor targetability of nanosized liposomes in tumor-bearing mice, *Macromol. Biosci.* 12 (2012) 849–856.
- [25] J.M. Harris, R.B. Chess, Effect of pegylation on pharmaceuticals, *Nat. Rev. Drug Discov.* 2 (2003) 214–221.
- [26] B.C. Tang, M. Dawson, S.K. Lai, Y.-Y. Wang, J.S. Suk, M. Yang, et al., Biodegradable polymer nanoparticles that rapidly penetrate the human mucus barrier, *Proc. Natl. Acad. Sci.* (2009).
- [27] P.A. Bird, D.P. Murray, M. Zhang, E.J. Begg, Intratympanic versus intravenous delivery of dexamethasone and dexamethasone sodium phosphate to cochlear perilymph, *Otol. Neurotol. Off. Publ. Am. Otol. Soc. Am. Neurotol. Soc. Eur. Acad. Otol. Neurotol.* 32 (2011) 933–936.
- [28] J. Zou, R. Sood, S. Ranjan, D. Poe, U.A. Ramadan, I. Pyykko, et al., Size-dependent passage of liposome nanocarriers with preserved posttransport integrity across the middle-inner ear barriers in rats, *Otol. Neurotol. Off. Publ. Am. Otol. Soc. Am. Neurotol. Soc. Eur. Acad. Otol. Neurotol.* 33 (2012) 666–673.